Regional Seismic Loss Assessment by Deep-Learning-based Prediction of Structural Responses

Taeyong Kim
Graduate Student, Dept. of Civil and Environmental Engineering, Seoul National University, Seoul, Korea

Junho Song
Professor, Dept. of Civil and Environmental Engineering, Seoul National University, Seoul, Korea

Oh-Sung Kwon
Associate Professor, Dept. of Civil and Mineral Engineering, University of Toronto, Toronto, Canada

ABSTRACT: As urban systems become more complex and sophisticated, the vulnerability of densely populated areas under earthquake hazard also increases. To establish risk-based strategies for hazard mitigation and recovery at the urban community level, many research efforts have been made for probabilistic seismic risk assessment (PSRA). When performing PSRA, structural responses are usually estimated by fragility functions or nonlinear static procedures. It is, however, noted that developing fragilities of each of numerous structures in a large area may require huge computational cost whereas nonlinear static procedures may not incorporate variabilities of the structural responses given a seismic intensity. Recently, the authors developed a deep-learning-based approach for probabilistic evaluation of the structural responses for a wide class of hysteretic behavior and ground motions. To reduce the computational cost of a regional seismic loss estimation and improve its accuracy, this paper proposes a new PSRA using the deep-learning-based method. To demonstrate the applicability of the proposed method and its merits, a hypothetical example of PSRA is investigated. In addition, this paper proposes a procedure to determine the optimal number of sensors, in which the deep-learning-based method is used to evaluate the seismic loss. Furthermore, the trained deep neural network model is employed as a surrogate model for a real-time PSRA. The deep-learning-based PSRA and the procedure to determine the sensors for installation are expected to improve PSRA at community level in terms of efficiency and applicability, and provide new insights into the seismic risk assessment and management of urban systems.

1. INTRODUCTION

Urban communities are relying on highly complex infrastructure systems with a large number of components and their interdependency. To properly assess the risk of an urban community against natural or man-made hazards, it is therefore important to predict not only the damage of each individual structural system but also the total loss at the community level. Due to various uncertainties in potential natural and man-made hazards, structural systems, and socio-economic impacts, the risk assessment of the urban community should be performed as a probabilistic analysis, for which simulation-based method is often used, e.g., Monte-Carlo simulation.

In order to predict the structural responses under an earthquake with the uncertainties incorporated, researchers have been using fragility functions developed for the structural systems of interest (Bai et al., 2009; Miller and Baker, 2015), while others adopted nonlinear static procedure (NSP) with probabilistic distributions assumed for the structural parameters (Goda and Hong, 2008). Both

methods are able to incorporate uncertainties into the predictions, but with some remaining challenges. In the former approach, a huge computational cost is required in developing the fragility functions for numerous types of structures based on the design spectrum of the region, and the ground motion scaling procedure during the fragility calculation may induce a bias in the response of nonlinear structures (Mai et al., 2016). On the other hand, the structural responses obtained from the existing NSP methods (ASCE 41-13, 2013; FEMA 440, 2005; Nassar and Krawinkler, 1991) cannot incorporate the uncertainties of the structural responses given seismic intensity measure and thus may show large estimation error, which eventually leads to under/overestimation of the regional seismic loss.

Recently, the authors developed a new framework to estimate the responses of a wide class of structural system using a deep learning method (Kim et al., accepted) and a Bayesian deep learning method (Kim et al., under review). It was found that the accuracy of the proposed method is superior to that of three existing simple methods which are widely used in practice: capacity spectrum method (FEMA 440, 2005), the R-μ-T method (Nassar and Krawinkler, 1991), and the coefficient method (ASCE 41-13, 2013). In order to improve the accuracy of the seismic regional assessment coping with the uncertainties of the structural responses, this research employs the *probabilistic* deep learning-based prediction framework (Kim et al. under review) instead of using an NSP method. The application of the proposed method will be demonstrated through numerical investigations. In addition, a deep-learning-based method is proposed to determine the required number of sensors for near-real-time assessment of the regional seismic loss after an earthquake event.

2. REGIONAL LOSS ESTIMATION USING DEEP LEARNING METHOD

This section briefly provides the background knowledge about the probabilistic seismic loss estimation of an urban community and the probabilistic deep neural network which was recently developed to estimate the nonlinear responses of single degree of freedom (SDOF) system. The procedure of the deep learning-based PSRA method is as follows: (1) ground motion intensity measures (IM) of the target region are derived from the ground motion prediction equation (GMPE), (2) structural responses are estimated by the probabilistic deep learning method (Kim et al. under review), (3) the corresponding regional loss is evaluated based on the estimated structural responses, and (4) iterate from step (1) to step (3) for each event simulation.

2.1. Probabilistic seismic risk assessment

A GMPE is usually written as follows: for an earthquake j at site i (Campbell and Bozorgnia, 2008)

$$\ln Y_{ij} = f\left(M_j, R_{ij}, \theta_i\right) + \sigma_{ij}\varepsilon_{ij} + \tau_j\eta_j \quad (1)$$

where Y_{ij} represents the IM, $f\left(M_j, R_{ij}, \theta_i\right)$ denotes the prediction of the median IM by the attenuation law as a function of magnitude M_j, seismological distance R_{ij}, and a set of other explanatory parameters θ_i, and ε_{ij} and η_j denote the intra- and inter-event residuals, respectively which are random variables of mean zero and standard deviation one. The levels of uncertainties in intra- and inter-event residuals are represented by standard deviations σ_{ij} and τ_j, respectively.

The probability that the loss caused by an event exceeds a threshold l is calculated as:

$$P(L \geq l) = \int P(L \geq l|\boldsymbol{y}) f_{\mathbf{Y}}(\boldsymbol{y})\, d\boldsymbol{y} \quad (2)$$

where $\boldsymbol{y}$ and $f_{\mathbf{Y}}(\boldsymbol{y})$ respectively denote the vector of the IMs at the locations of the individual structures and its joint probability density function (PDF). Using Eq. (1), Eq. (2) can be rewritten as:

$$P(L \geq l) = \sum_{s=1}^{S}[\lambda_s \int P(L \geq l|\boldsymbol{y}(M,R,\eta,\varepsilon)) \cdot f_{\mathbf{X}|s}(M,R,\eta,\varepsilon|s) dM dR d\eta d\varepsilon] \quad (3)$$

where λ_s denotes the annual occurrence rate of the event at source s, $\boldsymbol{y}(M,R,\eta,\varepsilon) = \boldsymbol{y}(\boldsymbol{x})$ represents Eq. (1), and $f_{\mathbf{x}|s}(\cdot)$ represents the

conditional joint PDF of the random vector $\mathbf{X} = \{M, R, \eta, \varepsilon\}$ given a seismic source s. Introducing the occurrence rates normalized by their sum $\lambda_t = \sum_{s=1}^{S} \lambda_s$, i.e. $\alpha_s = \lambda_s/\lambda_t$, and a predictive PDF $f_{\mathbf{X}}(\boldsymbol{x}) = \sum_{s=1}^{S} \alpha_s \cdot f_{\mathbf{X}|s}(\boldsymbol{x}|s)$, Eq. (3) can be rewritten as

$$P(L \geq l) = \lambda_t \cdot \int P(L \geq l|\boldsymbol{y}(\boldsymbol{x})) \cdot f_{\mathbf{x}}(\boldsymbol{x}) d\boldsymbol{x} \quad (4)$$

Then, the exceedance probability, or the complementary cumulative distribution function (CCDF) can be estimated by Monte Carlo simulation (MCS) as

$$P(L \geq l) \approx \lambda_t \cdot \frac{1}{N} \sum_{n=1}^{N} I(L \geq l|\boldsymbol{x}_n) \quad (5)$$

where $I(L \geq l|\boldsymbol{x}_n)$ is an indicator function which gives one if the regional loss for sample $\boldsymbol{x}_n$ generated with respect to $f_{\mathbf{X}}(\boldsymbol{x})$ exceeds the threshold l, and zero otherwise.

2.2. Probabilistic evaluation of seismic responses using deep learning method

To probabilistically estimate the responses of a nonlinear hysteretic system without compromising the accuracy, the authors recently developed the deep neural network-based prediction framework (Kim et al., under review). The deep neural network (DNN) model is designed to evaluate the *peak* transient displacement, which is the most important response from the earthquake engineering perspective. The architecture of the DNN model is depicted in Figure 1.

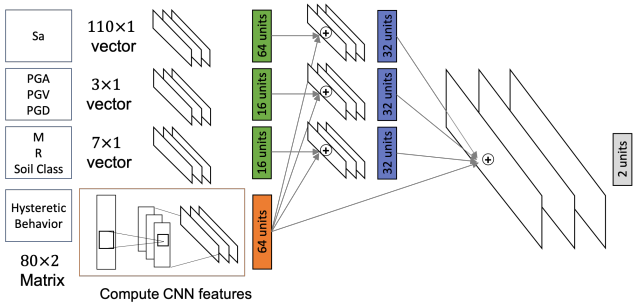

Figure 1: Schematic diagram of the probabilistic DNN model

The nonlinear seismic behavior of a structural system is represented by the hysteresis loops described in terms of force and displacement vectors. The features of the hysteretic behavior, that impact the inelastic seismic response of the structural system, are extracted by a convolution neural network (CNN), i.e. an orange box in Figure 1. The CNN has recently achieved practical success, especially in image classification and face recognition whose dataset shows strong spatial correlation. The hysteretic loop is obtained by performing a quasi-static cyclic analysis of an SDOF system using predefined displacement steps.

On the other hand, a set of useful features that can illustrate the intensities or characteristics of a stochastic ground motion excitation is used as the input of the DNN model. To this end, three different types of information are employed: source, peak values, and frequency contents of ground motions. Finally, using the Bayesian deep neural network scheme whose loss function is proportional to the negative logarithm of a Gaussian probability density function, the DNN model is developed to predict the conditional mean and variance of the structural responses given input features describing structure and ground motions.

In order to develop the DNN model, 54,090 hysteretic behaviors (Linear 90, Bilinear 27,000, and Bilinear with stiffness degradation 27,000), and 1,499 ground motions obtained from the NGA database (Power et al., 2008) are employed for training. For example, the predicted probabilistic peak displacement of a single structure under 1,499 ground motions are plotted in Figure 2 (rearranged in increasing order of the mean response predicted by the probabilistic model) along with the structural responses obtained by the time history analysis (blue circles). Note that the plot shows the natural logarithms of the peak displacements. The mean curve predicted with DNN model is plotted together with an orange-colored area representing mean ± 1 standard deviation (SD) interval, which covers approximately 70% of the probability distribution of the predicted structural response.

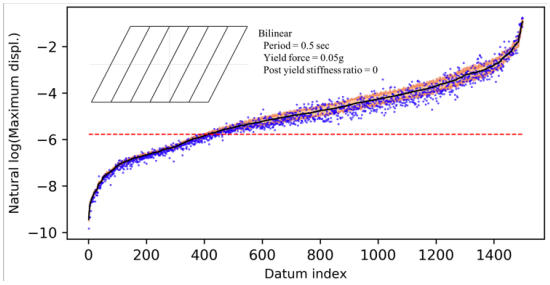

Figure 2: Performance of the probabilistic DNN model.

It is found that most of the data points fall within the mean ± 1SD intervals in Figure 2. It is also noteworthy that the width of the SD interval varies. In particular, the SD interval is relatively small and constant when the peak displacement is small, but it increases after passing the red horizontal line that corresponds to the yield displacement of the system. This is because a structural system behaves nonlinearly under a relatively large intensity ground motion, but the features that we used to train the probabilistic neural network partially describe the ground motion characteristics that may influence the nonlinear behavior of a structural system. This phenomenon indicates that the probabilistic DNN can successfully capture the uncertainties increased by the nonlinear behavior of the structure. Thus, using the DNN model, one can estimate the mean structural response under an earthquake the uncertainty associated with the predicted structural response.

3. AGGREGATED REGIONAL MONETARY LOSS

As a case study of regional loss assessment, we consider a set of hypothetical buildings which mimic a building stock in downtown Vancouver. The moment magnitude M_w 7.9 event from a point source located at $(48.9°\,\mathrm{N}, 123.2°\,\mathrm{W})$ is investigated. The set of 200 hypothetical buildings are randomly distributed over a square area of 2.5 km by 2.5 km whose center is located at $(49.2°\,\mathrm{N}, 123.2°\,\mathrm{W})$, as shown in Figure 3. 18 different building types associated with the HAZUS-Earthquake classification (FEMA and NIBS 2003; Goda and Hong, 2008) are introduced including 80 residential and 120 commercial buildings. The structural systems are approximately modeled as bilinear SDOF systems and the parameters of each building type are shown in Table 1.

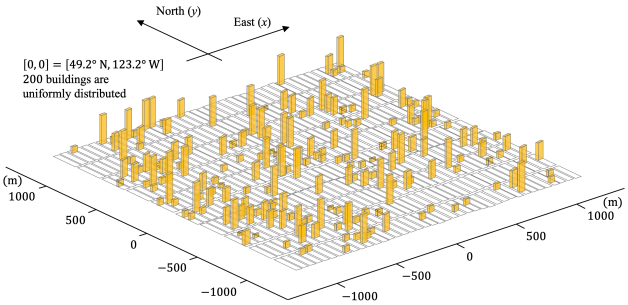

Figure 3: 200 buildings distributed on 400 property lots (40×10) in a virtual downtown area

3.1. Structural damage assessment and monetary loss estimation

Bilinear SDOF systems are investigated in a seismic design framework (NRCC 2005) in which the minimum required design base shear force V_d is given as

$$V_d = C_s \cdot W \tag{6}$$

where W represents the total weight of the structural system, and C_s denotes the design base shear coefficient of the given building type (Table 1). On the other hand, the yield displacement of the building Δ_y is given as

$$\Delta_y = R_N C_s W / k \tag{7}$$

where R_N is the coefficient representing the ratio between the actual yield strength of a designed structure to the design base shear V_d, and k represents the stiffness of the system. The ductility capacity μ_R and R_N are assumed to follow lognormal distributions with the mean values in Table 1 and the coefficients of variation (c.o.v) of 0.3 and 0.15 (Ellingwood et al., 1980; Ibarra, 2003), respectively.

By assuming that the monetary loss starts to occur as the building response exceeds the yield point of the hysteretic curve, the capacity and demand of the structural system are described in terms of the ductility ratio. Accordingly, the

Table 1: Damage cost information about hypothetical buildings (Goda and Hong, 2008).

I_{BT}[a]	# of bldgs.	# of stories	Size (m)	Structural & occupancy types	$L_{BL}(1)$, $L_{CO}(1)$, $L_{BI}(1)$ (CAD/ft^2)	$\beta_{BL}, \beta_{CO}, \beta_{BI}$	T_n (s)	Mean R_N	Mean μ_R	Target C_s[b]
1	8	2	10×12	W1-RES1	87.6, 21.9, 19.9	0.75, 0.68, 0.57	0.4	2	6	0.12
2	8	1	8×12	W1-RES1	87.6, 21.9, 19.9	0.75, 0.68, 0.57	0.4	2	6	0.12
3	17	2	15×30	W2-RES3	111.4, 27.9, 26.3	0.81, 0.68, 0.62	0.4	2	6	0.12
4	12	2	15×30	W1-COM1	47.8, 26.5, 23.9	0.81, 0.68, 0.43	0.4	2	6	0.12
5	1	5	18×36	S4M-RES3	111.4, 27.9, 26.3	0.69, 0.58, 0.53	0.7	2.25	4	0.1
6	2	5	18×36	S4M-COM4	103.5, 51.7, 163.9	0.70, 0.58, 0.57	0.7	2.25	4	0.1
7	1	13	18×36	S4H-RES3	111.4, 27.9, 26.3	0.69, 0.59, 0.53	1.4	2.25	3	0.075
8	1	13	18×36	S4H-COM4	103.5, 51.7, 163.9	0.70, 0.59, 0.57	1.4	2.25	3	0.075
9	7	2	15×30	C2L-RES3	111.4, 27.9, 26.3	0.76, 0.64, 0.58	0.4	2.5	6	0.12
10	10	2	15×30	C2L-COM1	47.8, 26.5, 23.9	0.75, 0.64, 0.41	0.4	2.5	6	0.12
11	18	5	18×36	C2M-RES3	111.4, 27.9, 26.3	0.75, 0.64, 0.58	0.6	2.5	5	0.12
12	27	5	18×36	C2M-COM4	103.5, 51.7, 163.9	0.77, 0.64, 0.62	0.6	2.5	5	0.12
13	13	15	18×36	C2H-RES3	111.4, 27.9, 26.3	0.76, 0.64, 0.58	1.65	3	3	0.05
14	25	15	18×36	C2H-COM4	103.5, 51.7, 163.9	0.77, 0.64, 0.62	1.65	3	3	0.05
15	4	2	15×30	URMLR-RES3	111.4, 27.9, 26.3	0.81, 0.69, 0.62	0.35	2	5	0.08
16	34	2	15×30	URMLR-COM1	47.8, 27.9, 26.3	0.81, 0.69, 0.43	0.35	2	5	0.08
17	4	3	20×40	URMMR-RES3	111.4, 27.9, 26.3	0.81, 0.69, 0.63	0.5	2	3.3	0.08
18	8	3	20×40	URMMR-COM2	61.0, 33.4, 19.5	0.80, 0.69, 0.49	0.5	2	3.3	0.08

[a] I_{BT} is the building index which is related to the structural and occupancy types defined in HAZUS-Earthquake (FEMA and NIBS, 2003)
[b] C_s is used to represent the seismic design level for existing buildings.
Note that 5% post-yield stiffness ratio is assumed for structural systems in this research.

damage factor δ due to a seismic excitation can be represented as (Goda and Hong, 2008)

$$\delta = \max\left(\min\left(\frac{\mu-1}{\mu_R-1}, 1\right), 0\right) \quad (8)$$

where μ represents the displacement of the system subjected to an earthquake (normalized by the yield displacement). Total collapse occurs when $\delta = 1$, while the partial damage is observed for $\delta \in (0, 1)$.

For convenience, the monetary seismic loss of the structural damage is categorized into three types in terms of the previously defined damage factor: building-related loss $L_{BL}(\delta)$, contents-related loss $L_{CO}(\delta)$, and business-interruption loss $L_{BI}(\delta)$ (Goda and Hong, 2008). Such loss functions are expressed as

$$L_*(\delta) = \delta^{\beta_*} L_*(1) \quad (9)$$

where $*$ can be BL, CO, and BI, δ is the damage factor calculated with Eq. (8), and β is the model parameter. $L_*(1)$ denotes the replacement costs of the complete damage state for each loss type in terms of Canadian dollar (CAD). These values are available in Table 1. By summing up the damage loss functions of all buildings in the target area, one can estimate the aggregated seismic loss subjected to the earthquake scenario as

$$L = \sum_{i=1}^{n_R}\left(L_{BL}(\delta_i) + L_{CO}(\delta_i) + L_{BI}(\delta_i)\right) \quad (10)$$

where n_R represents the total number of building in the region. The maximum possible seismic loss of the region is equal to L computed from Eq. (10) when $\delta_i = 1$ for all buildings.

3.2. Scenario earthquake

To estimate the IMs for each property lot given the assumed point source event, the GMPE suggested by Campbell and Bozorgnia (2008) is used in this numerical example, while the intra-event residuals are adopted from Loth and Baker (2011) to consider the correlations between both different intensities and locations. For simplicity, the soil properties at sites are described in terms of shear velocity $Vs_{30} = 760\ m/s$.

3.3. Numerical investigation

5,000 MCS are carried out to assess the seismic loss for 200 hypothetical buildings. Unlike the coefficient method, since the probabilistic DNN model provides the mean and variance of the structural responses for each scenario, the peak displacement of each building can be randomly generated using the estimated distribution parameters. First, in order to confirm the effects of the spatial correlation, the aggregated losses are

computed with and without considering such correlation. The exceedance probabilities $P(L \geq l)$ are computed for both cases as shown in Figure 4. The results confirm that the spatial correlation highly influences on the seismic loss assessment, especially where the systemic events have low probability, i.e. low and high aggregate loss. Therefore, one might over-or underestimate the probability of occurrence given regional seismic loss when neglecting such correlation.

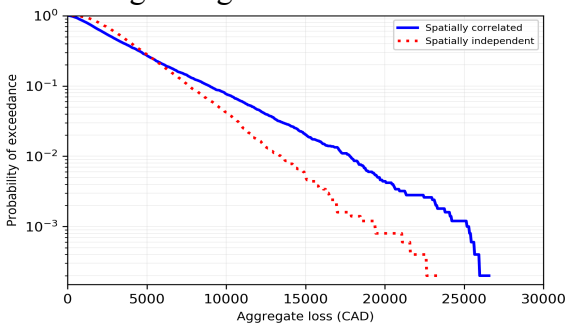

Figure 4: The effects of spatial correlation on aggregated regional losses

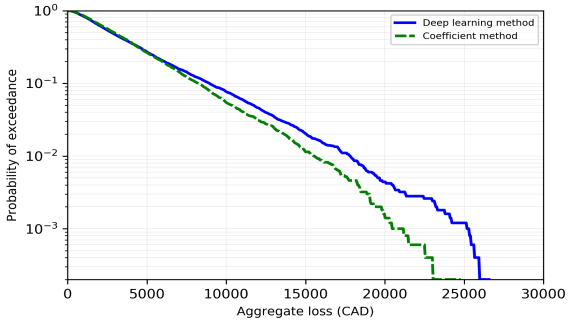

Figure 5: Comparison between the aggregated losses obtained from the probabilistic DNN model and the coefficient method

Next, to demonstrate the impact of the accuracy of structural response predictions, the aggregate loss obtained from the proposed method is compared with the one based on structural responses estimated by the coefficient method (ASCE 41-13, 2013; Figure 5). The exceedance probabilities match well when the aggregated loss is low, i.e. the peak displacement is formed around the yield displacement during excitation. However, as the intensity of the earthquake is increased, the discrepancy becomes severe, especially the loss evaluated using the coefficient method underestimates the damage of the region. This is because (1) the coefficient method predicts the peak displacement with a large error (Kim et al., accepted), and (2) it cannot incorporate the variabilities of the structural responses given IM. The results confirm that such uncertainties make a significant impact on the results of seismic losses and thus should be taken into account when performing PSRA.

4. FINDING OPTIMAL NUMBER OF SENSORS FOR NEAR-REAL-TIME ASSESSMENT

In prediction of regional seismic loss for future earthquake scenarios, IMs are simulated at every property lot using attenuation law. If one aims to use the proposed method for the purpose of near-real-time loss assessment based on data collected from the sensors in the region, the assessment should rely on limited number of sensors. In this study, a deep-learning-based method is proposed to find the optimal number of sensors for effective near-real-time regional loss assessment. The proposed procedure is summarized as follows:

- **Step 1**: Generate training and test datasets using a hypothetical earthquake scenario. For each event, generate IMs for property lots and estimate the corresponding loss.
- **Step 2**: Select a certain number of sensors in the region (randomly distributed), then estimate the IMs for the entire region by interpolation. For example, among 400 property lots, if 10 sensors are used, IMs for 390 property lots are estimated using a 2D linear interpolation. Moreover, to use the interpolation method, we always select the sensors located at the corner of the region.
- **Step 3**: After training the DNN model to predict the regional loss given IMs, calculate the error, e.g. mean squared error between prediction and actual value, using the test dataset.
- **Step 4**: Iterate from **Step2** to **Step 3** as varying the number of sensors.

As a result, the residual errors are plotted with respect to the number of sensors installed in the

area, which can be helpful for a stakeholder to find the optimal number of sensors to be installed.

To demonstrate the proposed procedure by the example of 200 hypothetical buildings investigated above, the DNN model which adopts CNN is constructed as shown in Figure 6. Since the IMs on 400 property lots (40 × 10) resemble a piece of image, CNN is considered a good choice to predict its seismic loss. Dropout (Srivastava et al., 2014) and Batch normalization (Ioffe and Szegedy, 2015) are applied after a rectified linear operator (ReLU; Nair and Hinton, 2010) for proper training.

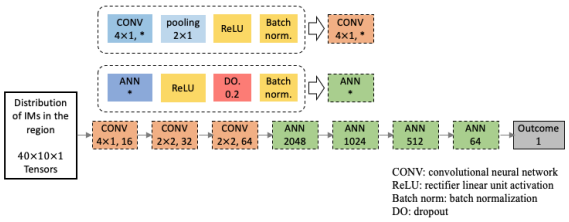

Figure 6: DNN model to predict the aggregated loss

To make the method simple and practical, only peak ground acceleration (PGA) for each grid is considered as our target IMs for input to predict the regional loss. 9 different numbers of installed sensors are considered: 5, 10, 15, 20, 40, 60, 80, 100 and 200 (i.e. 9 different DNN models are constructed), and 4,000 samples are used to train the DNN model among 5,000 samples generated from Section 3 (i.e. the remaining 1,000 samples are used for testing the DNN models after training). In order to resolve the skewness of the distribution, the natural logarithm is applied to the input. Adam optimizer (Kingma and Ba, 2014) is introduced as an optimization algorithm to minimize the mean squared error (MSE) with 64 batches and 2,000 epochs (Figure 7).

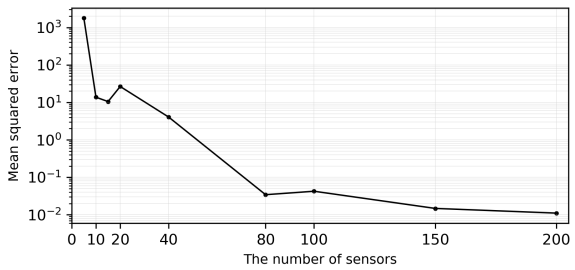

Figure 7: The number of sensors in the region and corresponding mean squared error

Even though the MSE of test set does not monotonically decrease as the number of sensors is increased, Figure 7 shows a clear trend. More specifically, the MSE has no significant changes until the number of sensors is increased up to 20. After that, the greater number of sensors are used, the faster MSE drops to the certain values, then slowly decreases after 80 sensors. Since the locations of the sensors are randomly selected in the region, the MSE can stay large even if the number of sensors is increased, especially where the number of sensors is relatively low.

Based on these results, the stakeholder can decide the minimum number of sensors as around 80 because a further increase is not expected to significantly improve the performance of the DNN model. Moreover, the trained DNN model can be used as a surrogate model as a replacement of the time-consuming MCS procedure. Therefore, using the proposed procedure and trained DNN model, seismic loss estimation can be carried out in near-real-time with the identified optimal number of sensors.

5. CONCLUSIONS

Using the probabilistic deep learning-based prediction of structural responses, a new regional seismic loss estimation method is developed. To check the applicability, a numerical investigation was carried out for a set of 200 hypothetical buildings located in a virtual downtown area. It was demonstrated that one can assess the regional loss using the deep learning method with considering the spatial correlation of intensity measures using the cross-correlation model. In addition, a procedure to determine the optimal number of sensors for the purpose of near-real-time regional loss assessment is proposed using the deep learning method. Using the proposed procedures and the developed deep learning model, stakeholders can decide the optimal number of sensors to be installed in the region to facilitate near-real-time regional seismic loss assessment. Although the identified optimal number of sensors can help stakeholder's decision, the information on optimal location per a given number of sensors is also desirable. To this end,

further study is currently underway using the probabilistic deep learning method.

6. ACKNWOLEDGEMENT

The first and the second author are supported by the project "Development of Life-cycle Engineering Technique and Construction Method for Global Competitiveness Upgrade of Cable Bridges" of the Ministry of Land, Infrastructure and Transport (MOLIT) of the Korean Government (Grant No. 16SCIP-B119960-01), and the third author is supported by the Korean Federation of Science and Technology Societies (KOFST) grant funded by the Korean government (MSIP: Ministry of Science, ICT and Future Planning). Finally, this research was enabled in part by support provided by WestGrid (www.westgrid.ca) and Compute Canada (www.computecanada.ca).

7. REFERENCES

ASCE (2013). "Seismic evaluation and rehabilitation of existing buildings.", ASCE/SEI 41-13 (Public Comment Draft), American Society of Civil Engineers, Reston, VA.

Bai J.W, Hueste M.B.D, Gardoni P. (2009). "Probabilistic assessment of structural damage due to earthquakes for buildings in Mid-America." *Journal of structural engineering*, 135(10), 1155-1163.

Campbell K, Bozorgnia Y. (2008). "NGA ground motion model for the geometric mean horizontal component of PGA, PGV, PGD and 5% damped linear elastic response spectra for periods ranging from 0.01 to 10 s." *Earthquake Spectra*, 24(1), 139-171.

Ellingwood B.R, Galambos T.V, MacGregor J.G, Cornell C.A. (1980). "Development of a probability based load criterion for American national standard A58." Washington, DC: National Bureau of Standards. National Bureau of Standards Special Publication No. 577.

Federal Emergency Management Agency and the National Institute of Building Sciences. (2003). "HAZUS-Earthquake: technical manual." Washington, DC: FEMA and NIBS.

FEMA. (2005). "Improvement of nonlinear static seismic analysis procedures." Report No. FEMA-440, Washington, DC.

Goda K, Hong HP. (2008). "Estimation of seismic loss for spatially distributed buildings." *Earthq. Spectra*, 24: 889–910.

Ibarra L.F. (2003). "Global collapses of frame structures under seismic excitations." Ph.D. thesis, Stanford University, Stanford, CA.

Ioffe S, Szegedy C. (2015). "Batch normalization: accelerating deep network training by reducing internal covariate shift." ArXiv150203167 Cs.

Kim T, Kwon OS, Song J. "Seismic response prediction of nonlinear structural systems with deep neural networks." *Neural Networks*, accepted.

Kim T, Song J, Kwon OS. "Probabilistic evaluation of seismic responses using deep learning method." under review.

Kingma D.P, Ba J. (2014). "Adam: A method for stochastic optimization." ArXiv14126980 Cs.

Loth C, Baker J.W, (2011). "A spatial cross-correlation model of spectral accelerations at multiple periods." Earthq *Eng Struct Dyn,* 42: 397–417.

Mai C, Konakli K, Sudret B. (2017). "Seismic fragility curves for structures using non-parametric representations." *Front. Struct. Civ. Eng.*, 11(2): 169–186.

Miller M, Baker J.W, (2015). "Ground-motion intensity and damage map selection for probabilistic infrastructure network risk assessment using optimization." *Earthquake Engineering & Structural Dynamics*, 44(7): 1139–1156.

Nair V, Hinton GE. (2010). "Rectified linear units improve restricted boltzmann machines." *In Proc. 27th International Conference on Machine Learning*.

Nassar A, Krawinkler H. (1991). "Seismic demands for SDOF and MDOF systems." John A. Blume Earthquake Engineering Center Report No. 95, Stanford University, CA.

NRCC. (2005). National Building Code of Canada 2005. Ottawa, Canada: NRCC.

Power M, Chiou B, Abrahamson N, Bozorgnia Y, Shantz T, Roblee C. (2008). "An overview of the NGA Project." *Earthq. Spectra* 24, 3–21.

Srivastava N, Hinton G, Krizhevsky A, Sutskever I, Salakhutdinov R. (2014). "Dropout: a simple way to prevent neural networks from overfitting." *J. Machine Learning Res.* 15, 1929–1958.